IEEE Robotics and Automation Letters (RA-L) paper, presented at ICRA 2024, Yokohama, Japan. Cite as RA-L paper.

Variable Grounding Flexible Limb Tracking Center of Gravity for Sit-to-Stand Transfer Assistance

Sojiro Sugiura[1], Jayant Unde[1], Yaonan Zhu[1], and Yasuhisa Hasegawa[1]

***Abstract*—Wearable robotic limbs support sit-to-stand (STS) transfer with increased stability while maintaining a compact size, as well as providing body weight support. This paper proposes a new robotic limb, Variable Grounding Flexible Limb (VGFL). The VGFL achieved a novel strategy in which its grounding point tracks the forward shift of the wearer's center of gravity (CoG) during STS. Since the strategy keeps the distance between the grounding point and the CoG close, an upward force can efficiently work for the STS assistance. To implement the strategy, this paper utilized the High-Strength and Flexible Mechanism (HSFM). The HSFM can change its grounding point while being capable of lifting body weight with one motor. Owing to these unique characteristics, the VGFL can realize the strategy without multiple actuators and complex controllers. Furthermore, real-world experiments confirmed that the grounding point of the VGFL accurately tracked the forward shift of the CoG during the STS assistance. Moreover, experiments conducted with three healthy subjects showed that the VGFL reduced the surface myoelectricity of the lower limbs during STS transfer. The VGFL could demonstrate high support performance in STS with the CoG tracking strategy.**

***Index Terms*—Wearable Robotics, Physically Assistive Devices, Mechanism Design, STS transfer, CoG tracking**

I. Introduction

Sit-to-stand (STS) transfer, such as standing up from a bed or toilet bowl, is an activity of daily living (ADL). However, it is difficult for elderly people and physically challenged patients to perform. In particular, STS was reported to be one of the most difficult tasks in using a toilet [1] and determines whether a person can complete the excretion process alone. The success of STS movement involves several factors, such as maximum lower-limb muscle power, postural sway, and psychological condition [2], [3], which are common problems for elderly people and mobility-impaired patients. Because STS failure leads to falling and serious accidents [4], assistance for successful STS is in great demand.

Several assistive devices for STS movement have been developed. Some devices are integrated with a robotic caster walker and can support both STS and walking [5], [6]. Providing the user with sufficient area of support, they contribute to the stability of STS movements. These devices can be used in hospitals and large nursing care facilities. However, due to their size, these devices are less practical for use in individual homes and smaller facilities.

In contrast, wearable-type robots are compact and can be used in a variety of situations [7], [8], [9]. These assistive devices are worn on the lower limbs and apply torque to the knee and hip joints using actuators. However, the risk of falling remains because the support area of the user is not expanded. Therefore, there is a need for STS assistive devices that are compact and expand the support polygon.

Supernumerary Robotic Limbs (SRL) [10], [11], [12], [13], [14] have been developed for the assistance of ADL and fulfill two key requirements: they are worn by the user and expand the support area. When assisting in STS, the two limbs, which are attached to the waist, touch the ground and gradually extend to lift the wearer. SRL can reduce the risk of falls due to its large support polygon. However, SRLs have limitations in terms of providing efficient force for STS assistance.

In the case of assistance by SRL, the upward assistive force is not always high. The force decreases as the user proceeds to STS and eventually reaches zero in the standing posture [12]. This is because the upward force needs to be reduced so that the limbs do not slip on the ground. The slip would be caused because the vertical projection of the CoG shifts away from the limbs' grounding point as the STS proceeds. This paper proposes a novel strategy to provide a continuous higher support force: the grounding point of the limb is movable over the ground and keeps it close to the CoG.

One complicated solution to achieve the strategy is shown in the left parts of Fig. 1. This system controls actuators based on the CoG detected by sensors. It requires constant control of three actuators: a linear actuator, the rotation angle of the waist, and the rotation of the wheel. Simultaneously, to capture the CoG position, cameras or wearable IMUs (inertial measurement unit) should be prepared.

In this paper, we approached this problem by utilizing the High-Strength and Flexible Mechanism (HSFM) [15], [16], as shown in the right part of Fig. 1. The HSFM rolls on the ground and has the potential to track the CoG mechanically with only one actuator. The HSFM changes its shape between a straight and spiral pose with one motor and wires (Fig. 2). This transformation enables the HSFM to roll on the ground and change its grounding point. Additionally, the HSFM is strong enough to lift a human owing to its mechanical constraints. Due to its unique mechanism, the HSFM can

Manuscript received: August 10, 2023; Accepted October 12, 2023.

This paper was recommended for publication by Editor Jee-Hwan Ryu. Jee-Hwan Ryu upon evaluation of the Associate Editor and Reviewers' comments. This work has been supported by JST Moonshot RD, Grant No. JPMJMS2034 Japan

[1]All Authors are with the Department of Micro-Nano Mechanical Science and Engineering, Nagoya University, Nagoya 464-8601, Japan sugiura@robo.mein.nagoya-u.ac.jp

Digital Object Identifier (DOI): see top of this page.

IEEE Robotics and Automation Letters (RA-L) paper, presented at ICRA 2024, Yokohama, Japan. Cite as RA-L paper.

IEEE Robotics and Automation Letters (RA-L) paper, presented at ICRA 2024, Yokohama, Japan. Cite as RA-L paper.

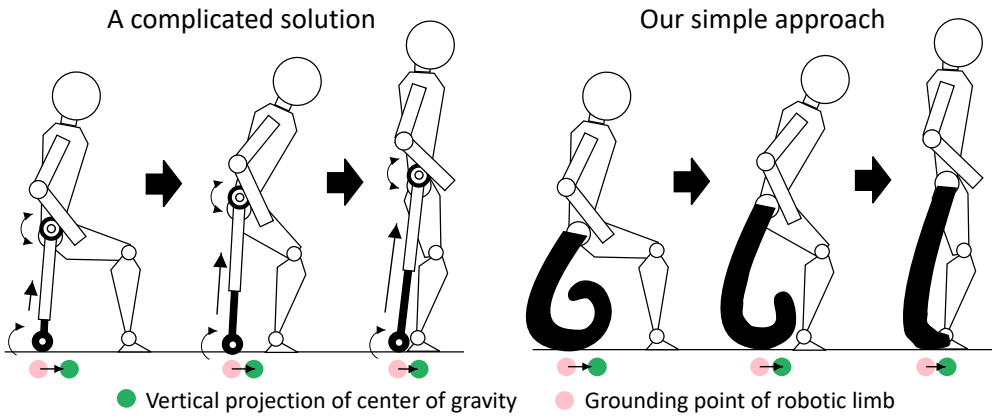

Fig. 1. Illustration showing one complicated solution vs our simple proposed strategy. The grounding point of the limb tracks the vertical projection of the CoG of the wearer.

achieve our strategy with no more than one actuator, without complex controllers, and without sensors. This could be a very simple solution to make limbs' grounding point movable on the ground while being capable of lifting the user's weight. However, the movement of the HSFM and humans should be carefully analyzed to achieve the CoG tracking function. Therefore, this paper aims to develop a wearable robotic limb with the HSFM, elucidate the CoG tracking function, and evaluate its effectiveness for STS assistance.

The main contributions of this study are as follows.

1) A wearable limb-type robot Variable Grounding Flexible Limb (VGFL), incorporating the High-Strength and Flexible Mechanism (HSFM), was developed.
2) To the best of the authors' knowledge, this is the first strategy to mechanically track the wearer's CoG during STS.
3) The function of CoG tracking was evaluated in the real world and could contribute to a sufficient assistive force.
4) Experiments with three healthy subjects to verify the effectiveness of STS assistance were conducted by measuring surface-myoelectricity and showed promising results.

In the following section of this paper, the mechanism and control system of the robot are introduced in Section II. Following that, analysis and experiments to achieve the CoG tracking function are conducted in Section III. Further, the performance of the VGFL on STS assistance is evaluated using myoelectric values in Section IV. Finally, the limitations and future plans are discussed in Section V.

II. Variable Grounding Flexible Limb (VGFL)

This section describes the design of the proposed robot Variable Grounding Flexible Limb (VGFL).

A. Mechanical design

The VGFL, as shown in Fig. 2, assists the wearer in performing ADL while changing its grounding points.

Two HSFMs are attached to the right and left waists: Fig. 2 (a). The VGFL has six degrees of freedom (DoF) in total. In the waist, pitch and yaw joints are attached, and one DoF in each HSFM (Fig. 2 c). The VGFL achieves various assistance tasks by controlling the joints and shifting the grounding points. However, since this paper focuses on the HSFM and the assistance of STS transfer, the pitch and yaw angles are minimally explained. The weight of the VGFL is 14.5 kg.

The length parameters of the mechanism were determined based on general body parameters [17], [18]. The height of the HSFM changes in the range of 460–1000 mm. Its minimum height (460 mm) was determined to be lower than the height of the waist in the sitting posture, and the maximum height (1000 mm) was determined to be higher than that of the waist in the standing posture. The position of the pitch joint was designed to be equivalent to that of the user's hip joint. The pitch joint can move similarly to the hip joint of the wearer. In addition, the yaw angle can move similarly to the lateral and medial rotations of the hip joint.

B. Driving systems

Each DoF of the VGFL is driven with a brushed DC motor. The driving mechanism and control systems are shown in Fig. 2 (c)–(f).

One HSFM mechanism is controlled with one DC motor and four wires (Fig. 2 d). Two wires pass around the perimeter of the HSFM and work to uncoil it [16]. The other wires pass around the inner circumference of the HSFM and operate to wind up it. The outer wire must transmit high-tension force to lift body weight. Hence, the pulleys to pull up the outer wires are directly driven by the DC motor. Pulleys for coiling rotate in conjunction with the pulleys for uncoiling via a synchronous belt. The synchronous belt pulley's gear ratio is designed to be capable of controlling two kinds of wires with one DC motor. The motor is a Maxon motor (333975, 90W, and gear ratio 1:23). The driving system was designed to lift 30 kg per one HSFM and the motor. Based on the previous article [16], the required tension force [kgf] to lift a certain weight [kgf] is represented as

$$(Tension force) = 1.63 \times (Weight) \quad (1)$$

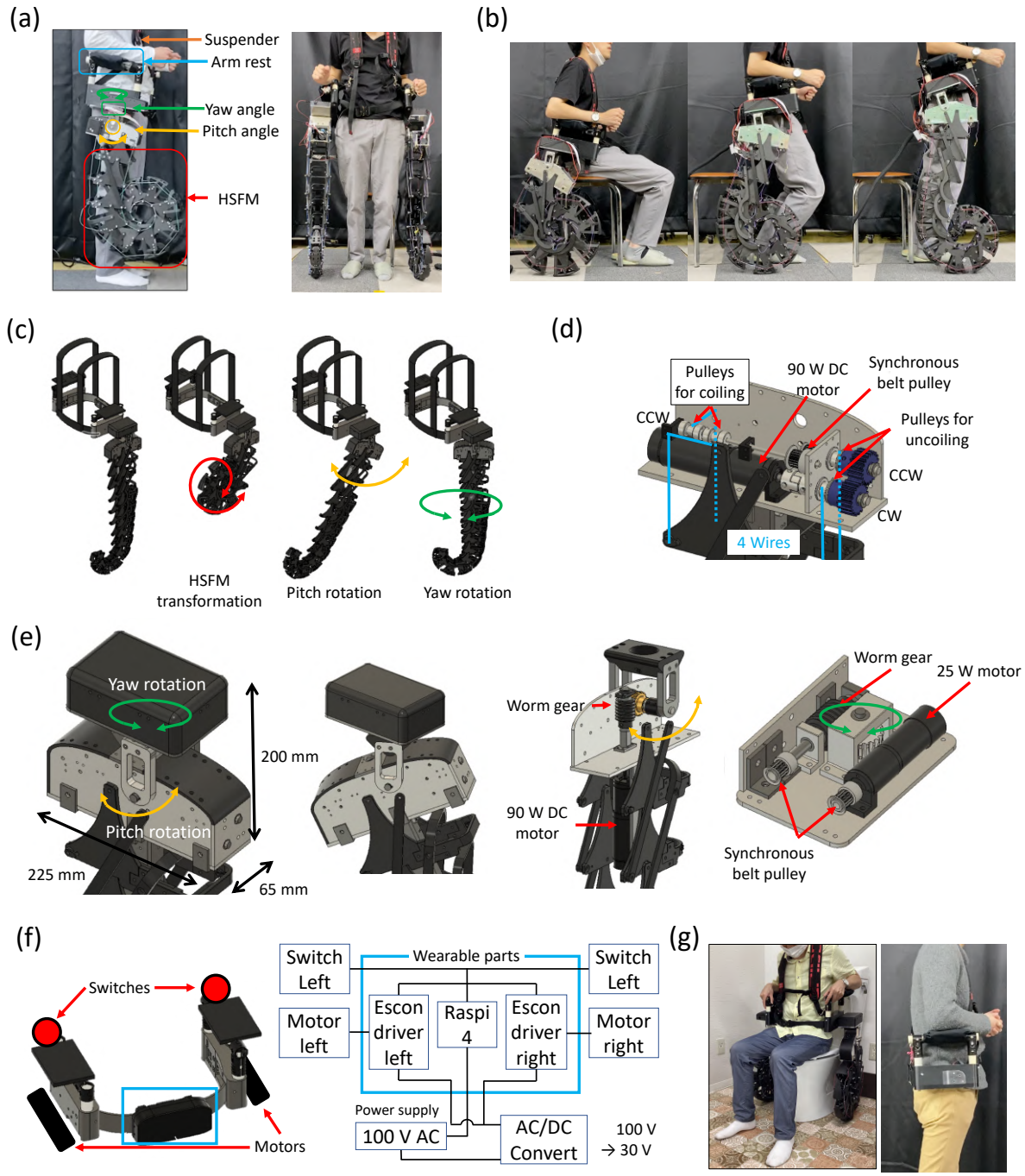

Fig. 2. Variable Grounding Flexible Limb (VGFL). (a) Overview of the robot and mechanical parts. (b) Sit-to-stand assistance. (c) 3 DoF: HSFM transformation, pitch, and yaw. (d) Wire driving mechanism of the HSFM. (e) Pitch and yaw rotation mechanism. (f) Control systems. (g) Wearing segments.

Then, the required force to lift 30 kg is 48.9 kgf (479 N). Given that the radius of the pulleys was designed 7 mm, the required torque generated by the motor is 3.35 Nm. This torque can be generated by the DC motor. The allowable torque of the gear box is 3.8 Nm, which is strong enough to lift body weight.

The pitch rotation is controlled with one DC motor and a set of worm gear. The motor is the same Maxon motor (333975, 90W, and gear ratio 1:23). The motor is placed into the HSFM, contributing to its downsizing (Fig. 2 e). The gear ratio of the worm gear is 1:10. The worm gear is housed in the same box as the gear and motor for the HSFM. An advantage of a worm gear is a self-lock function: It rotates only in the forward direction from the motor, preventing back driving from external forces. The motor does not need to be continuously driven when supporting static weight.

The yaw rotation is controlled with one DC motor, a set of worm gear, and a synchronous belt (Fig. 2 e). The motor is a Maxon motor (333975, 25W, and gear ratio 1:23). The motor and the worm gear are connected with a synchronous belt for its downsizing. The gear ratio of the worm gear is 1:10.

TABLE I
STATUS OF THE HSFMS BY CONDITIONS OF THE SWITCHES.

Left switch	Right switch	Status of the HSFMs
OFF	OFF	Supporting
OFF	ON	Lifting
ON	OFF	Coiling
ON	ON	Supporting

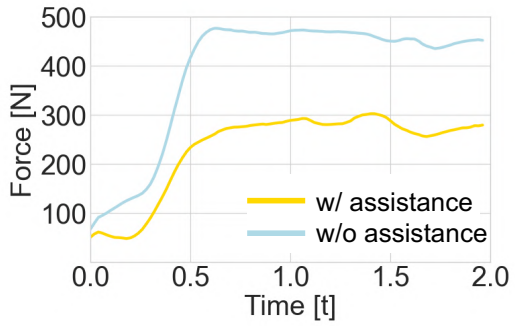

Fig. 3. Total feet reaction force. The yellow line represents the force applied with the assistance of the VGFL. The blue line shows that without the VGFL.

Fig. 2 (f) shows the control system of the VGFL. The motors are controlled with Maxon's drivers (ESCON). ESCON drivers control the speed of rotations with high accuracy based on feedback from an encoder. The main computer is Raspberry Pi 4, sending commands to the drivers. Triggers of the commands are switches attached to the wearing segment. The switches express ON or OFF and work as shown in Tab. I. When only pushing the right switch, the right and left HSFMs move and lift the body weight. When only the left switch is on, the motor moves to make the HSFM a spiral pose (toward sitting). In the other conditions, the motors keep a certain angle and enable the HSFMs to support the body weight. The speed of the motor was predetermined and can be changed by sending a command to Raspberry Pi 4 from another computer.

C. Wearable parts

The VGFL is worn using a waist belt and a suspender (Fig. 2 a). The belt is covered by an aluminum frame mounting the HSFM. The frame performs the role of a rigid body that conveys body weight to the HSFM and transfers assistance forces to the body. Elbow rests are used to support the user's body weight. There were also other ideas to support the user's weight using the underarms or buttocks. However, pressing on the underarms is detrimental to blood flow. In addition, because the VGFL focuses on assisting various ADLs, such as using a toilet (Fig. 2 g), the buttocks could not be selected as the weight-bearing segment. Furthermore, hemiplegic patients have difficulty moving their arms and supporting the body weight with the elbow on their own. Therefore, collaboration with body-holding mechanisms [19] is required for the future work.

D. Lifting

We experimented to verify the capacity of body weight support in STS. The individual utilized a foot plantar pressure measurement system (Pedar) [16]. The signals were recorded at a sampling frequency of 50 Hz and then subjected to smoothing using a moving average technique within 0.1-second intervals. The subject performed STS movement for 2 seconds in two conditions: with the assistance of the VGFL and without wearing the VGFL.

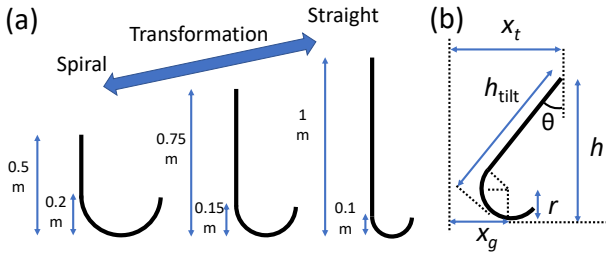

Fig. 4. A model of the HSFM. (a) Change in radius as per height. (b) Calculation parameters when the HSFM tilts.

Fig. 3 shows the time-series data of the foot force (total of both feet). The blue line shows the force during proceeding with STS without the VGFL. The force significantly increased after leaving the chair (at 0.5 s). The peak was 475 N and expressed the weight of the person. In contrast, the force was reduced by the VGFL. As shown in the yellow line, the peak of the force was 300 N when using the VGFL.

This experiment clarified that the VGFL sufficiently reduced the reaction force applied from the ground to the foot. In the case where the grounding points are fixed at a predetermined position, the reaction force gradually decreases as the STS process proceeds [12]. Hence, this measurement results showed that the VGFL could assist the STS movements while maintaining the upward assistance force. This favorable result could be attributed to the effectiveness of the CoG tracking strategy.

One HSFM is capable of supporting 20 kg [16], but the reduced foot pressure was less than the capacity. This is because a certain amount of weight must remain on the feet to maintain the balance.

III. CoG TRACKING

The HSFM has the potential that its grounding point mechanically tracks the forward shift of CoG during STS transfer. In this section, the tracking function is analyzed based on the measured movements of the HSFM and humans. Further, the accuracy of the tracking is evaluated in real-world experiments.

A. Parametric analysis

This section analyzes the postural trajectory of STS transfer and the movement of the HSFM to estimate the tracking accuracy. The trajectory of the top of the HSFM was measured using an optical motion capture system (OptiTrack). The HSFM was driven using the wires and the DC motor. Meanwhile, the trajectory of the human body segments and CoG was measured with an IMU motion capture system (Xsens). The position of the segments and the CoG was automatically calculated on Xsens software.

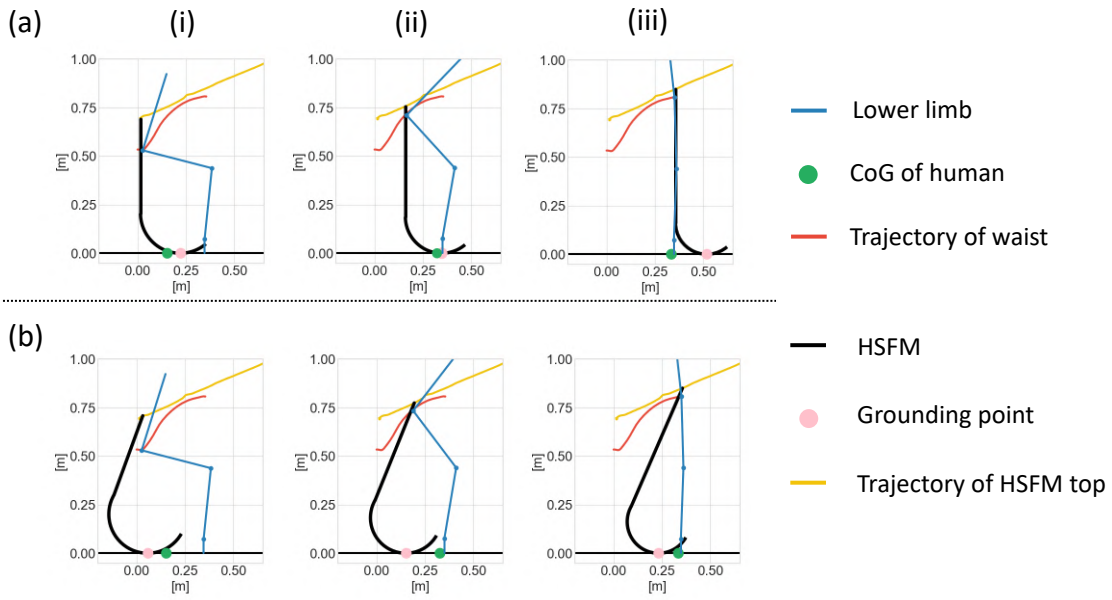

Fig. 5. Measured trajectory of humans and the HSFM. The process of STS was separated into three phases (i)–(iii) in this paper. (a) shows the simulation of STS assistance when the HSFM does not tilt. (b) shows that when the HSFM tilts.

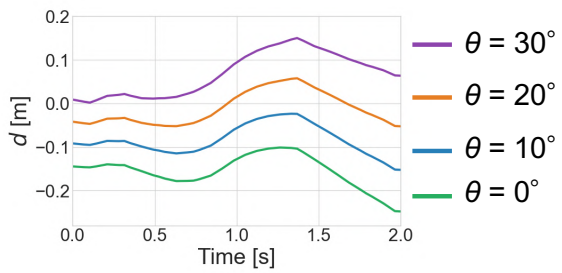

Fig. 6. Distance d between the grounding point and the CoG under four conditions: $\theta = 0, 10, 20, 30°$.

To simulate the movement of the grounding point, we built a model of the HSFM, as shown in Fig. 4 (a). The parameters of this model are the height of the HSFM and the radius of the spiral segment. When the height is 500 mm, the radius is 200 mm. The radius linearly increases according to the height. When the HSFM tilts, the grounding point changes and can be calculated based on the following equations and Fig. 4 (b). The distance between the grounding point and the origin is donated as x_g:

$$x_g = x_t - (h_{\mathrm{tilt}} - r)\sin\theta + r\cos\theta \tag{2}$$

where x_t, h_{tilt}, r, and θ mean a distance from the origin to the top of the HSFM, the height of the HSFM, the radius of the HSFM's spiral segment, and the tilted angle of the HSFM. h_{tilt} and r can be represented using h:

$$h_{\mathrm{tilt}} = \{h - r(1 - \cos\theta + \sin\theta)\}/\cos\theta \tag{3}$$

$$r = -h_{\mathrm{tilt}}/5 + 0.3 \tag{4}$$

h referees to the measured trajectory of the HSFM's top: yellow lines in Fig.5.

Fig. 5 shows the human model, the CoG, the HSFM model, the grounding point, and trajectories of the waist and the top of the HSFM. We compared these movements and discussed the detailed methodology of CoG tracking. Fig. 5 (a) shows a simple illustration with the upright HSFM (θ = 0). Fig. 5 (b) shows a tilted HSFM (θ = 30) for better CoG tracking. In this paper, the STS movement was separated into three phases: (i) just after leaving the chair, (ii) middle of STS, and (iii) completing STS.

First, the grounding point of the HSFM should be behind the wearer's CoG just after leaving the chair. Fig. 5 (a-i) shows that the grounding point was not behind the CoG. This situation increases the risk of a backward fall because the CoG is outside the support polygon formed by the device and the wearer. To prevent this, we made the HSFM tilt 30° backward, as shown in Fig. 5 (b-i), which made the grounding point positioned backward.

Second, the grounding point should be still behind the CoG of the wearer in the middle of STS to prevent a backward fall. Since Fig. 5 (a-ii) shows that the grounding point was in front of the CoG, tilting was required. Fig. 5 (b-ii) illustrated that the grounding point can be behind the CoG by tilting the HSFM.

Finally, after completing the STS, putting the grounding point nearby CoG can be helpful to support the standing posture. The situations that both Fig. 5 (a-iii) and (b-iii) show could be better.

We calculated the distance between the grounding point and the CoG under multiple angle conditions: $\theta = 0, 10, 20, 30°$. The distance d can be calculated

$$d = x_{\mathrm{CoG}} - x_{\mathrm{g}} \tag{5}$$

where x_{CoG} means the distance between the vertical projection of the CoG and the origin.

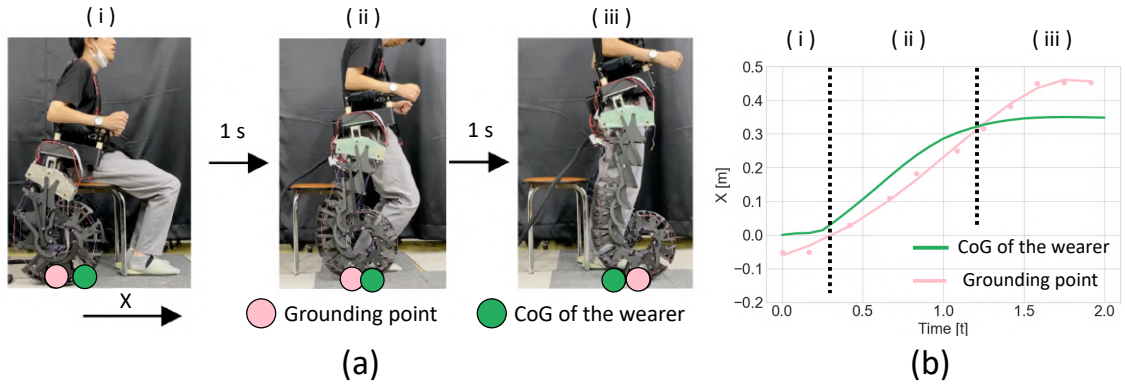

Fig. 7. The trajectory of the CoG of the wearer and the grounding point of the VGFL were measured. (a) The scenario of assisting in STS shows the vertical projection of the CoG and the grounding point. (b)The time-series data of the position of CoG and the grounding point. The vertical axis x was defined as the distance from the initial position of the CoG in the forward direction.

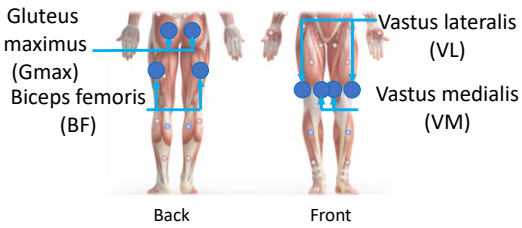

Fig. 8. Measured muscles in the experiment of Sec. IV.

x_g is referred by Fig. 4 (b). The shapes of the time series data were the same for all conditions, but the initial position differs. To prevent backward fall during phase (i) and (ii), the grounding point should be behind the vertical projection of the CoG. The situation is observed only when θ is 30°. However, during 1.0 – 1.5 s, the CoG in the case $\theta = 20^\circ$ was closer to the grounding point than that of $\theta = 30^\circ$. The ideal approach is to be capable of changing θ during STS support. However, since a large torque is applied to the pitch angle θ during STS transfer, it requires a high torque-producing motor. Because large motors significantly lower the VGFL's usability, we have decided to tilt the angle of the HSFM by 30° and keep it during the assistance.

B. Evaluation

In this section, the trajectories of the grounding point and the CoG during the STS assistance are measured, and the strategy of CoG tracking is evaluated. The trajectory of the CoG of the wearer was measured using Xsens. The wearer performed STS transfer for 2 seconds with the assistance of the VGFL. The movement of the HSFM was measured using OptiTrack. Markers of OptiTrack were attached to each grounding part of the HSFM and displayed when each part touched the ground. From the results of the analysis and calculation, the time-series data of the grounding position were obtained as approximate curves of the third order.

Fig. 7 shows how the position of the grounding point and the CoG shifted during STS. At process (i), the grounding point was located behind the CoG. This indicates that the VGFL prevented backward falling in the sitting posture. In the middle stage of assistance (ii), the gradients of the two lines were almost the same, indicating that the grounding point could track the CoG. Therefore, the wearer can avoid backward falls. In addition, the distance between the grounding point and the vertical projection of the CoG was always less than 15 cm. Hence, the wearer can efficiently obtain an upward assistive force. However, the shift of the CoG stopped at the latter part of the assistance, and the grounding point overtook the CoG by 10 cm. This result was not expected in Section III-A (see Fig. 5 b-iii), but owing to this overtaking, the VGFL could reduce the risk of falling forward in the standing position.

The results in the real world were different from the simulated results (see Fig. 6). The difference would come from the characteristics of human movement. In the real world, without the VGFL, the CoG was in a support area of the feet to prevent falling. However, with the VGFL, as the wearer's weight was placed on the VGFL, the CoG shifted toward the VGFL. Additionally, the pose of the VGFL could cause the difference. The angle of the arm rest changed during STS, as shown in Fig.7 (a). This happened because the attachment between the VGFL and the wearer was weak. Therefore, the development of a better fitting attachment to the human body is required [19].

IV. Experiment

This section examines the effectiveness of the VGFL on muscle effort, based on experiments with healthy subjects.

A. Participants and Procedures

The subjects were three young men without physical disabilities (24.7±1.2 years, 170±4.0 cm, 64.3±5.1 kg). Consent was obtained from all participants before performing the experiments. In addition, this study was approved by the Ethics Committee of Nagoya University (No. 22-16). Although the VGFL is intended to assist elderly people in the future, this paper focused on experiments with only healthy subjects to verify the basic assistive effectiveness of the proposed device.

The subjects performed STS transfer with and without the VGFL. The duration of the motion was unified to 2.0 s. The

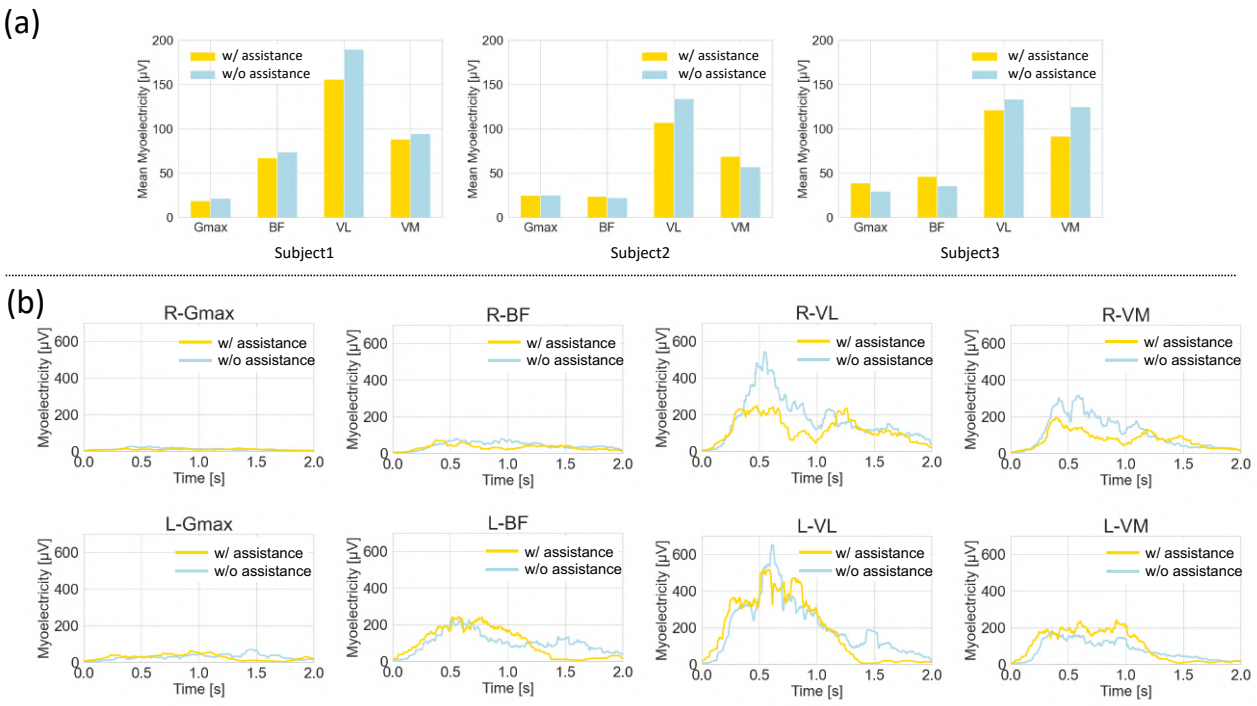

Fig. 9. Experiment results. (a) Averaged myoelectricity output by each muscle during 2-second sit-to-stand movement. The outputs of the right and left muscles are averaged. The yellow and blue bars represent the output with and without the assistance of the VGFL, respectively. (b) Time-series data of myoelectricity in the eight muscles of subject 1. R and L denote the right and left muscles, respectively.

subjects practiced completing the movement at the same speed with that of unassisted STS. They chose preferred constant speed of the motor to complete the task. The trigger to initiate support was held by the wearer.

B. Measurements

The myoelectric potential was utilized to evaluate muscle effort when using the VGFL [20]. This value enables quantitative evaluation of the performance of the robot. In this experiment, the surface myoelectric potential was measured using a wireless sensor (Cometa). The acquired signals (2000 Hz) were smoothed using the root mean square (RMS) with a time window of 0.1 s [20], [9].

The following muscles, shown in Fig. 8, were measured on the right and left sides: gluteus maximus (Gmax), biceps femoris (BF), vastus lateralis (VL), and vastus medialis (VM). These muscles were selected based on articles about STS assistance devices [5], [7], [21], [22], [23].

C. Results & Discussion

Fig. 9 (a) presents the mean myoelectricity levels for each muscle during STS, revealing variations in effort among different muscle groups. The VL muscles required the largest effort in all subjects, followed by the VM muscles. These muscles are responsible for the extension of the knee joint, which is performed during STS [24]. The muscle activity of them were reduced by the assistance of the VGFL. The average reduction rate in the VL and VM muscles was 13.2%. This reduction is assumed to be achieved by body weight support. Since the VGFL supported the weight partially, the required extension torque of the knee was reduced. The mean myoelectricity represents the burden of repeating an exercise. Hence, it was confirmed that the VGFL could reduce the load on the VL and VM muscles when repeating STS transfer. On the other hand, some muscles were activated more, such as the subject2's VM muscle. This would occur because individuals vary in muscle use. This is not a major issue because the averaged data of VL and VM muscles shows a reduction, which means the total effort was relieved.

In contrast, the output of the BF and Gmax muscles was less than that of the VL and VM muscles. The BF muscles flex the knee joint. Because flexion of the knee joint is not performed during STS, it is valid that the BF muscles were not used as much. The Gmax muscles extend the hip joint, which should be necessary for STS. However, it has been reported that the output of the Gmax muscle is small in the context of STS [24]; therefore, we did not observe a large output of the Gmax muscle or a corresponding reduction.

Fig. 9 (b) shows the time-series data of the myoelectricity of subject 1 during STS. The VL and VM muscles output large voltages, and the time taken to reach the peak in these muscles was 0.5 s. These results are considered valid, as this tendency was also reported by Roebroeck [24]. The peak voltage in the right VL muscle was reduced by 54% owing to the assistance. Additionally, the peak in the left VL muscle was reduced by 21%. Although the right VM muscle shows reduced activity, that of the left represents an increase. This increase is not a critical issue because the average values for left and right show a reduction, and there is no significant increase in

the maximum output of the L-VM muscle. This may have occurred due to the subject's weight being shifted towards the left leg. An individual cannot perfectly distribute their weight evenly between the left and right legs. The maximum output determines whether a person can perform activities. The VGFL successfully reduced the peak value of the most active muscles, implying that the VGFL may enable elderly people who cannot complete STS by themselves to perform STS.

In the future, experiments with the elderly and mobility-impaired patients will be necessary, as the VGFL has been designed to assist them.

V. Conclusion

Variable Grounding Flex Limb (VGFL), which changes the grounding points according to the assistance scenario, was proposed. This paper focuses on the assistance of STS movements using a novel strategy in which the grounding point of the VGFL mechanically tracks the forward shift of the wearer's CoG. This strategy was realized by the unique characteristics of the High-Strength and Flexible Mechanism (HSFM): The HSFM rolls on the ground with one motor while being strong enough. Due to its uniqueness, the VGFL achieved the CoG tracking function with a single degree of freedom and without complicated control systems. Additionally, real-world experiments have shown that the grounding point of the VGFL adequately tracked the wearer's CoG. The VGFL could achieve a sufficient support force for STS transfer because the force point acted near the CoG. Further, experiments to evaluate the effectiveness of the VGFL for STS assistance were conducted with three healthy subjects and showed sufficient reductions of the VL and VM muscle activities. These results indicate that the VGFL demonstrated high support performance of STS by realizing the CoG tracking function with the HSFM.

We adjusted the posture of the HSFM for more accurate CoG tracking. In the future, the tracking accuracy will be enhanced by changing the HSFM's geometric parameters. Additionally, we will also develop a system that changes the VGFL poses according to the physique of the wearer. Simultaneously, appropriate control method to enhance the effectiveness of the device will be investigated. Another limitation of this paper is the HSFM's volume. The HSFM is designed to lift the wearer, so the size of the robot becomes significant. The present VGFL might disturb other activities such as walking. Therefore, we will develop a more compact HSFM while maintaining its strength in the future. The compact limbs will improve the usability of the VGFL and enable it to assist in several ADLs such as walking.

References

[1] E. Kawanabe, M. Suzuki, S. Tanaka, S. Sasaki, and T. Hamaguchi, "Impairment in toileting behavior after a stroke," *Geriatrics & Gerontology International*, vol. 18, no. 8, pp. 1166–1172, 2018.

[2] S. R. Lord, S. M. Murray, K. Chapman, B. Munro, and A. Tiedemann, "Sit-to-stand performance depends on sensation, speed, balance, and psychological status in addition to strength in older people," *The Journals of Gerontology Series A: Biological Sciences and Medical Sciences*, vol. 57, no. 8, pp. M539–M543, 2002.

[3] P. B. Thapa, P. Gideon, R. L. Fought, M. Kormicki, and W. A. Ray, "Comparison of clinical and biomechanical measures of balance and mobility in elderly nursing home residents," *Journal of the American Geriatrics Society*, vol. 42, no. 5, pp. 493–500, 1994.

[4] B. Najafi, K. Aminian, F. Loew, Y. Blanc, and P. A. Robert, "Measurement of stand-sit and sit-stand transitions using a miniature gyroscope and its application in fall risk evaluation in the elderly," *IEEE Transactions on biomedical Engineering*, vol. 49, no. 8, pp. 843–851, 2002.

[5] J. Huang, S. Yan, D. Yang, D. Wu, L. Wang, Z. Yang, and S. Mohammed, "Proxy-based control of intelligent assistive walker for intentional sit-to-stand transfer," *IEEE/ASME Transactions on Mechatronics*, vol. 27, no. 2, pp. 904–915, 2021.

[6] T. C. Bulea and R. J. Triolo, "Design and experimental evaluation of a vertical lift walker for sit-to-stand transition assistance," *Journal of medical devices*, vol. 6, no. 1, 2012.

[7] W. Huo, H. Moon, M. A. Alouane, V. Bonnet, J. Huang, Y. Amirat, R. Vaidyanathan, and S. Mohammed, "Impedance modulation control of a lower-limb exoskeleton to assist sit-to-stand movements," *IEEE Transactions on Robotics*, vol. 38, no. 2, pp. 1230–1249, 2021.

[8] A. Tsukahara, R. Kawanishi, Y. Hasegawa, and Y. Sankai, "Sit-to-stand and stand-to-sit transfer support for complete paraplegic patients with robot suit hal," *Advanced robotics*, vol. 24, no. 11, pp. 1615–1638, 2010.

[9] S. Sugiura, Y. Zhu, J. Huang, and Y. Hasegawa, "Passive lower limb exoskeleton for kneeling and postural transition assistance with expanded support polygon," *IEEE/ASME Transactions on Mechatronics*, 2023.

[10] F. Parietti and H. Asada, "Supernumerary robotic limbs for human body support," *IEEE Transactions on Robotics*, vol. 32, no. 2, pp. 301–311, 2016.

[11] F. Parietti and H. H. Asada, "Supernumerary robotic limbs for aircraft fuselage assembly: body stabilization and guidance by bracing," in *2014 IEEE International Conference on Robotics and Automation (ICRA)*. IEEE, 2014, pp. 1176–1183.

[12] L. Treers, R. Lo, M. Cheung, A. Guy, J. Guggenheim, F. Parietti, and H. Asada, "Design and control of lightweight supernumerary robotic limbs for sitting/standing assistance," in *International Symposium on Experimental Robotics*. Springer, 2016, pp. 299–308.

[13] X. Wu, H. Liu, Z. Liu, M. Chen, F. Wan, C. Fu, H. Asada, Z. Wang, and C. Song, "Robotic cane as a soft superlimb for elderly sit-to-stand assistance," in *2020 3rd IEEE International Conference on Soft Robotics (RoboSoft)*. IEEE, 2020, pp. 599–606.

[14] J. Guggenheim, R. Hoffman, H. Song, and H. H. Asada, "Leveraging the human operator in the design and control of supernumerary robotic limbs," *IEEE Robotics and Automation Letters*, vol. 5, no. 2, pp. 2177–2184, 2020.

[15] X. Liu, C. Wang, and J. M. McCarthy, "The design of coiling and uncoiling trusses using planar linkage modules," *Mechanism and Machine Theory*, vol. 151, p. 103943, 2020.

[16] S. Sugiura, J. Unde, Y. Zhu, and Y. Hasegawa, "High-strength and flexible mechanism for body weight support," *ROBOMECH Journal*, vol. 10, no. 1, pp. 1–12, 2023.

[17] P. De Leva, "Adjustments to zatsiorsky-seluyanov's segment inertia parameters," *Journal of biomechanics*, vol. 29, no. 9, pp. 1223–1230, 1996.

[18] C. E. Clauser, J. T. McConville, and J. W. Young, "Weight, volume, and center of mass of segments of the human body," Antioch Coll Yellow Springs OH, Tech. Rep., 1969.

[19] T. Takahashi, M. Watanabe, K. Tadakuma, N. Saiki, K. A. M. Konyo, and S. Tadokoro, "Inflated bendable eversion cantilever mechanism with inner skeleton for increased payload holding," *arXiv preprint arXiv:2202.04270*, 2022.

[20] K. Tomohiro, M. Tadashi, K. Tohru, and S. Tsugutake, "Practical usage of surface electromyogram," *Biomechanism Library*, 2006.

[21] W. Huo, S. Mohammed, Y. Amirat, and K. Kong, "Active impedance control of a lower limb exoskeleton to assist sit-to-stand movement," in *2016 IEEE international conference on robotics and automation (ICRA)*. Ieee, 2016, pp. 3530–3536.

[22] M. A. Alouane, W. Huo, H. Rifai, Y. Amirat, and S. Mohammed, "Hybrid fes-exoskeleton controller to assist sit-to-stand movement," *IFAC-PapersOnLine*, vol. 51, no. 34, pp. 296–301, 2019.

[23] A. L. Kulasekera, R. B. Arumathanthri, D. S. Chathuranga, R. Gopura, and T. D. Lalitharatne, "A low-profile vacuum actuator (lpvac) with integrated inductive displacement sensing for a novel sit-to-stand assist exosuit," *IEEE Access*, vol. 9, pp. 117 067–117 079, 2021.

[24] M. Roebroeck, C. Doorenbosch, J. Harlaar, R. Jacobs, and G. Lankhorst, "Biomechanics and muscular activity during sit-to-stand transfer," *Clinical Biomechanics*, vol. 9, no. 4, pp. 235–244, 1994.